Nuclear Instruments and Methods in Physics Research A 856 (2017) 139–146

Contents lists available at ScienceDirect

Nuclear Instruments and Methods in Physics Research A

journal homepage: www.elsevier.com/locate/nima

The TwinEBIS setup: Machine description

M. Breitenfeldt[a], R. Mertzig[a,b], J. Pitters[a,d], A. Shornikov[a,c], F. Wenander[a,*]

[a] CERN, Geneva 23 CH-1211, Switzerland
[b] Technische Universität Dresden, 01069 Dresden, Germany
[c] GANIL, Bd. Becquerel, BP 55027, 14076 Caen Cedex 05, France
[d] Technische Universität Wien, 1040 Vienna, Austria

ARTICLE INFO

Keywords:
EBIST
EBIT
Charge breeder
Highly charged ions
Electron beam simulations

ABSTRACT

TwinEBIS is an Electron Beam Ion Source (EBIS) recently made operational at CERN. The device is similar in construction to the REXEBIS charge breeder operating at the ISOLDE facility. After relocation of the solenoid from the Manne Siegbahn Laboratory (MSL) Stockholm, TwinEBIS was commissioned at CERN and serves as a test bench dedicated to manipulation of low-energy highly charged ions. In this paper we give an overview of the setup and present advanced numerical simulations of the electron optics. In addition, the alignment procedure of the solenoid magnetic field is described and measurement results are presented. Results from cathode investigations, electron beam tests and ion extraction modulation are presented in a follow-up paper.

1. Introduction

The REXEBIS [1] pioneered the use of EBIS technology for charge breeding of radioactive beams. The versatile concept providing near contamination free beams, described in detail elsewhere [2,3], is the following: the REXEBIS charge breeder receives a pulsed 1^+ radioactive ion beam from a gas-filled Penning trap cooler and buncher and increases the charge state to an A/q-ratio in the 2.5–4.5 range in REXEBIS. The charge bred ions are then re-accelerated by the post-accelerating REX-ISOLDE linac [4,5] for nuclear physics experiments [6].

The success of the concept motivated several groups to pursue a similar approach for re-accelerated Radioactive Ion Beams (RIBs) such as the charge breeders Re-A EBIS at MSU-NSCL [7], CARIBU at Agronne National Lab [8], the ARIEL project at TRIUMF [9] or EBIS CB at RISP [10]. In parallel EBISes delivering highly charged stable ions such as RHIC EBIS at Brookhaven National Lab [11] made substantial progress. Being one of oldest operational EBISes among the major accelerator facilities, REXEBIS represents the previous generation of charge breeders that is presently being outperformed in terms of electron optics by most of the modern EBIS devices in a comparable role [12]. An upgrade would help REXEBIS to remain competitive and benefit the ISOLDE user community through increased performance.

In order to fully take advantage of the ongoing upgrade [13] of the ISOLDE re-acceleration complex, improved performance of the charge breeder is necessary [14]. The main direction is to provide a lower A/q-ratio in order to benefit from higher acceleration energy in the individually phased cavities of the superconducting part of the linac and to provide pulses with higher repetition rate (50 Hz) also for heavier elements. The former requires an elevated electron-beam energy (from present 4.5 to 10 keV) to strip electrons with higher binding energies. The latter calls for higher electron-current density (from present 150 to >1000 A/cm^2) in the breeder. Neither should compromise the output ion beam purity or the reliability of the setup.

The REXEBIS charge breeder is operational from early April until mid-December, dictated by the CERN injector schedule, either providing radioactive beams for experiments or stable beam for the linear accelerator tests. As such, the opportunities for machine studies, especially the ones requiring internal access to the EBIS, are limited. The latter is due to a single vacuum volume and a desired vacuum level in the 10^{-11} mbar range, requiring a full bake-out cycle of at least 10 days. To address the hardware development topics an EBIS test bench was introduced in 2014, based on an essentially identical copy of REXEBIS. At this device, called TwinEBIS, we do have the possibility to perform in-depth cathode and electron beam studies, including invasive modifications to the setup.

The increase of current density is addressed in two ways on two time scales. The first short-term approach is an incremental increase with minimum intervention by the introduction of new cathode materials and designs of the electron gun without changing the gun compression principle (magnetic compression only, i.e. immersed flow). This work includes also such aspects as maintaining long-term reliability by counteracting cathode poisoning and mechanical failures.

* Corresponding author.
E-mail address: fredrik.wenander@cern.ch (F. Wenander).

http://dx.doi.org/10.1016/j.nima.2016.12.037
Received 11 November 2016; Received in revised form 18 December 2016; Accepted 21 December 2016
Available online 23 December 2016

This kind of upgrade will allow REXEBIS to approach present day EBISes working with the same optics principle, such as RHIC EBIS or CARIBU. For immersed flow optics the electron current density in the trapping region is defined by the emission current density from the cathode and the maximum magnetic field. Equipping REXEBIS with IrCe cathodes [15] will allow reaching the state-of-the-art emission current density. Given the 2 T maximum field of the REXEBIS iron-shielded magnet, the device may achieve a current density of approximately 200 A/cm^2, which is comparable to more recent EBISes taking into account stronger magnets of the new machines: RHIC EBIS 5 T/525 A/cm^2 [16], CARIBU 6 T/750 A/cm^2 [17], RISP 6 T/target 505 A/cm^2 [10]. If the REXEBIS magnet is kept, a further performance upgrade is in principle only possible with a change of beam compression method to a combination of electrostatic and magnetic compression known as Brillouin optics [18].

In the longer run TwinEBIS is being prepared to host a prototype electron gun with a Brillouin compression scheme presently being developed [19] for a high frequency (200–400 Hz) C^{6+} source in cancer radiotherapy. With this new gun current densities in excess of 1000 A/cm^2 could be possible, allowing REXEBIS even with the present magnet to surpass the modern immersed flow optics EBISes. As the gun is being developed with a 5 T magnet option in mind, a future magnet upgrade at REXEBIS would put the breeder in line with the most ambitious EBIS projects presently aiming to combine Brillouin optics, high magnetic field and several amperes electron beams, such as Re-A EBIS [7] and ARIEL EBIS [9] at TRIUMF.

In this paper the mechanical design of TwinEBIS and its auxiliary equipment are described. Thereafter electron beam simulations are presented. Finally, the magnetic field alignment method for the solenoid and results thereof are given. Our results on several additional topics such as cathode investigations, electron beam test and ion extraction modulation are reported elsewhere [20].

2. Description of the TwinEBIS setup

Until 2011 the solenoid of TwinEBIS remained at MSL and served as a test bench for development of Electron String Ion Sources (ESIS) [21]. After the ESIS program was concluded, the solenoid with auxiliary vacuum equipment was transferred to CERN. Upon arrival at CERN the solenoid was re-commissioned. Major efforts were dedicated to improve the helium holding time in the magnet cryostat and to map and align the magnetic field. Thereafter TwinEBIS was built up and the first electron beam was launched in summer 2014.

2.1. Concept and mechanical design

The mechanical design of TwinEBIS is in general identical to REXEBIS and the unit even serves as a backup in case of major REXEBIS failure. The magnets are identical, although the modifications of the two cryostats are slightly different. The electron gun design is the same, but different cathode-to-anode distances have been tried at TwinEBIS. Also the internal structure is identical, apart from TwinEBIS having two more trapping tubes than REXEBIS. Complementary information about the REXEBIS design can be found in [22,23]. Here we give a brief overview of TwinEBIS and describe some of the key features, see Fig. 1.

Most EBIS setups feature a gate valve separating the electron gun volume from the trapping volume. This is not the case for REXEBIS/TwinEBIS as the electron gun is located at the very edge of the magnet iron shield, meaning that a retractable gun design with a bellow etc. would be required if a gate valve was to be introduced. Such a solution was deemed too complicated at the time of construction.

2.2. Electron gun

The TwinEBIS electron gun is of a semi-immersed type, with the cathode located at an intermediate field strength B of 0.2 T. The current density compression follows B^n (n~1), yielding a moderate compression factor of 10 in full 2 T field. The main drawback is a limited current density determined mainly by the maximum loading current density from the cathode. A lanthanum hexaboride (LaB_6) single crystal cathode with < 310 > orientation was chosen for its advantageous work function, that is claimed to be 2.41 eV [24].

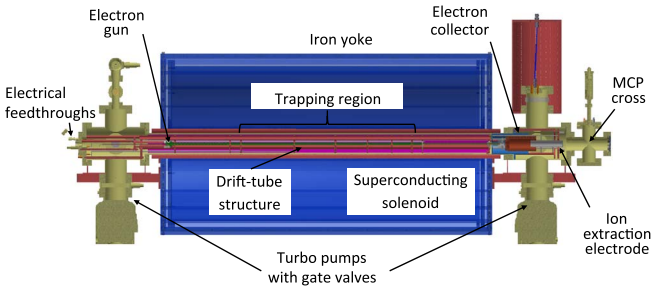

Fig. 1. Cross-section of the TwinEBIS setup with the essential elements being indicated. Just as for REXEBIS, TwinEBIS features a warm-bore iron-shielded 2 T superconducting solenoid. The electron gun is not separable from the trapping region with a vacuum valve.

The Wehnelt electrode with a 2.0 mm hole surrounds the 1.6 mm diameter cathode. The angle between Wehnelt surface and beam axis is 67°. The anode tip is located at a distance of 1.35 mm from the cathode surface and the hole size is 2.25 mm. The Wehnelt and anode electrodes are assembled with 0.5″ steatite isolators. Directly after the anode electrode the beam enters the first drift tube, which is on the same potential as the anode. Recently added precision pins between the two electrodes assure an alignment accuracy in the order of 20 μm. Schematic drawings of the electron gun are given in Fig. 2.

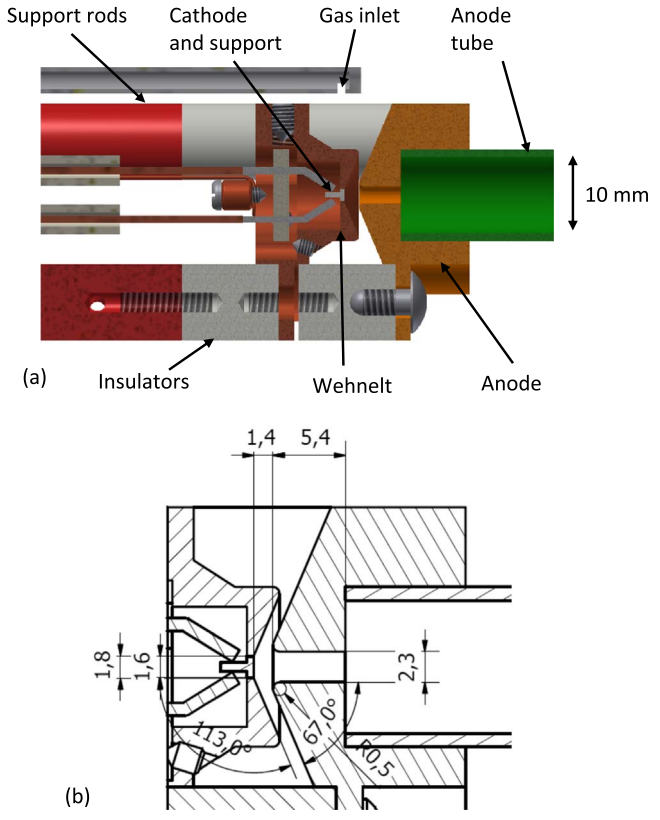

Fig. 2. Cross-section of the semi-immersed TwinEBIS electron beam gun. Its symmetry is three-fold and based around a 1.6 mm diameter LaB_6 cathode. The gas tube is for introduction of oxygen gas in order to remove poisoning compounds on the cathode surface.

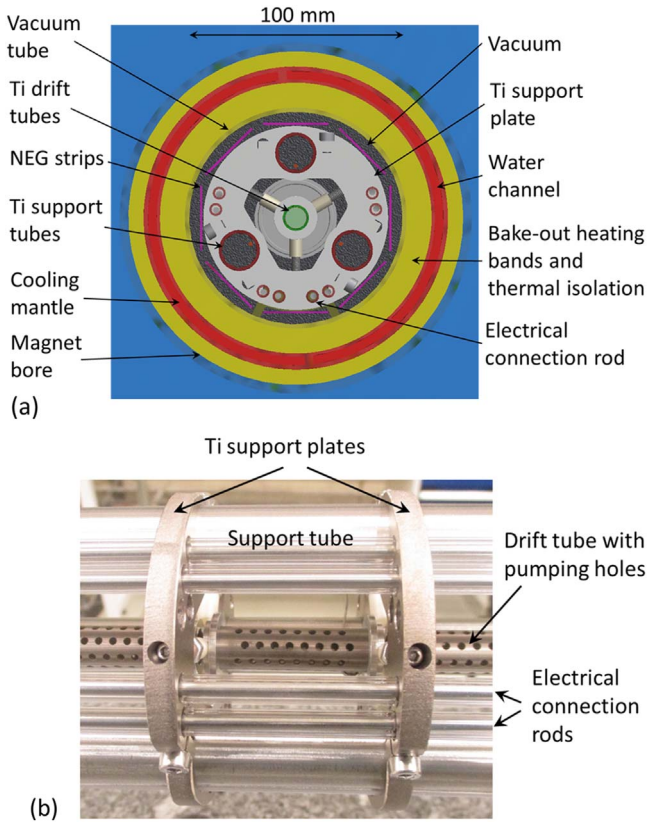

Fig. 3. (a) Transverse cross-section of the drift-tube structure with surrounding cooling mantle and magnet bore. (b) Photo of the drift-tube structure taken from the side, showing a short barrier drift tube.

2.3. Central region structure

TwinEBIS has five trapping tubes of lengths 89 mm, 120 mm, 146 mm, 189 mm and 246 mm located in the full magnetic field and at room temperature, which are axially enclosed by inner and outer barrier drift tubes. All drift tubes are made of titanium and have inner and outer diameters of 10 mm and 12 mm, respectively. The drift tube walls are perforated by 2 mm holes in a 4×4 mm pattern to improve pumping (compare Fig. 3b). At the end of the drift tubes no lossy sleeves to damp possible RF excitation [25] are installed, but the tubes are merely separated by 2 mm gaps in order to optimise the pumping. The drift tube alignment system allows to adjust the position of individual drift tubes with an accuracy of 80 ± 30 μm relative to the central axis as demonstrated by tests. The inner structure is confined in a 100 mm diameter vacuum tube of stainless steel. A cross-section view perpendicular to the beam axis and a side-view photo of the drift tube structure are shown in Fig. 3.

Outside the vacuum tube heating bands are placed. Thermal isolation and a cooling mantle ensure protection of the magnet while baking out the central vacuum tube at temperatures as high as 300 °C. With the TwinEBIS operating parameters of 0.5 A electron current at 5 keV electron energy and a trapping length of 0.8 m, the charge storing capacity is $6{\cdot}10^{10}$ elementary charges. The approximate potential depression, with respect to the drift tube, is 750 V and the difference in potential between the centre and the edge of the beam is 107 V.

2.4. Collector

The collector, made of oxygen-free high thermal conductivity (OFHC) copper, has a cylindrical absorbing surface and is magnetically shielded by a 5 mm thick screen of ARMCO® iron, see Fig. 4. The

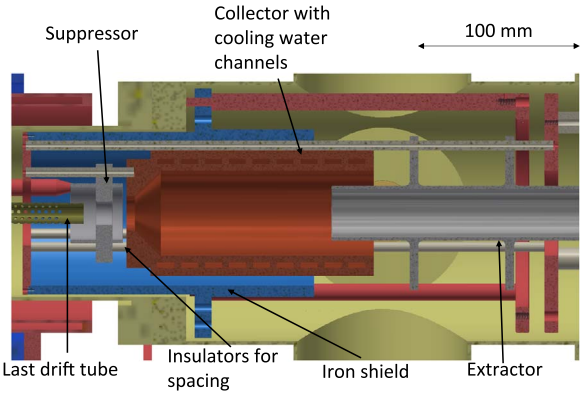

Fig. 4. Cross-section of elements in the electron collector region.

magnetic field inside the collector is reduced to < 0.02 T, enabling the electron beam to expand and be absorbed by the collector. The collector is water cooled through a two-way spiralling cooling channel with cross-section 3 mm·6 mm and a total length of ~1.6 m. The collector assembly is bakeable to > 300 °C. The average load current on the surface is < 8 mA/cm^2 and for a total power deposition of 1000 W the temperature increase is estimated to be < 2 K.

The collector does not have a conical absorption surface, which is usually the case in EBISes, but a cylindrical surface. The extractor, typically at −6.5 kV with respect to the collector, has a diameter of 28 mm. By having an extraction hole this large, we expect to minimise the ion beam aberrations; besides the pumping conductance increases. The drawback is a higher fraction of elastically reflected primary electrons, see Section 4.

2.5. Solenoid

The magnetic field of the solenoid from Oxford Instruments compresses and guides the electron beam from the gun to the trapping region. The magnet is shielded with a yoke of iron bars and has a warm bore, i.e. the drift tube structure is kept at room temperature. A liquid nitrogen jacket surrounds the helium cryostat, and both are refilled at 8 and 12 d intervals, respectively.

The field straightness specifies the maximal radial deviation from the geometrical axis of the magnetic field line passing the geometrical centre of the magnet. For a 0.5 A, 5 keV beam with a 0.5 mm diameter, a 0.1 mm displacement corresponds to a potential well difference of only 1 V between the displaced and non-displaced beams.

The field homogeneity denotes the variation in longitudinal field strength. A fluctuating field strength along the z-axis leads to a varying beam radius, which in turn modulates the beam potential according to:

$$\frac{\Delta U_{axis}}{U_{axis}} = \frac{\Delta B_{trap}}{B_{trap}} \cdot \frac{1}{2\ln\left(\frac{r_{tube}}{r_{ebeam}}\right) + 1}$$

where U_{axis} and B_{trap} denote axial beam potential with respect to the drift tubes and magnetic field in the trapping region, respectively. If as above a potential variation $\Delta U_{axis} < 1$ V is accepted, where $U_{axis} = -750$ V for TwinEBIS at nominal operating condition, the homogeneity has to be better than 1%. The magnet specification of < 0.3% inside the 800 mm trapping region is well within this limit. To avoid magnetic field disturbances only non-magnetic materials have been used inside the vacuum system, except for the iron shield around the collector.

2.6. Vacuum system

For a charge breeder system the vacuum requirements are very strict as the number of injected ions can be outnumbered by ions from

the residual gases by orders of magnitude, even for very good UHV [26].

Special care has been taken in the selection of materials. Only stainless steel 316 LN or 316 L (vacuum chamber and support rods), OFHC copper (electron gun and collector), ARMCO® (iron shielding for collector), titanium (drift tubes and inner structure support), Al_2O_3, steatite and quartz tubes (isolation of electrical leads and electrodes) and CuBe (electrical connectors) have been used. In the external beam diagnostics vacuum-cross also Macor® and Kapton® coated wires are found. The stainless steel and ARMCO® have been vacuum fired at 950 °C and 900 °C, respectively, to evacuate mainly H_2 from the bulk material. The Al_2O_3 was heat treated at 1000 °C in atmosphere.

The system is baked out for 48 h at full temperature, which ranges from 150 °C for valves and the beam diagnostics cross, over 250 °C for the gun and collector crosses to 300 °C for the bore tube surrounding drift tubes and non-evaporable getters (NEG). A staged ramping up avoids saturation of the passively activated NEG strips.

In Fig. 1 the vacuum system is indicated. The backbone in the pumping system consists of two 180 l/s two-stage turbo-molecular drag pumps TPU 180 H DN 100CF from Balzers-Pfeiffer with exceptional compression ($N_2 > 1{\cdot}10^{12}$) and attainable base pressure ($< 5{\cdot}10^{-12}$ mbar). The turbo pumps are backed by a smaller turbo pump (Pfeiffer Vacuum TSU261), which in turn is pumped by an oil-based roughing pump. Around the inner structure, St707 NEG strips [27] from SAES Getters S.P.A are mounted in an octagonal geometry. These passively activated NEG strips with a total surface close to 6500 cm^2 have a H_2 pumping speed of > 3000 l/s, while O_2, N_2 and CO are pumped with 65%, 15% and 40% of this speed. Inert gases are not pumped.

After some hundred hours beam conditioning the pressure readouts in the gun and collector cross are low 10^{-11} and high 10^{-11} mbar, respectively, even with the electron beam launched. The pressure in the actual trapping region has not been established, but it is expected to be better than at REXEBIS which is connected to a transfer line from a buffer-gas filled Penning trap and a mass separator, that both have 2–4 orders of magnitude worse pressures than the EBIS itself. The total pressure in the REXEBIS trap has been estimated from the extracted beam to be in the low 10^{-11} mbar region [2].

Oxygen, and other gases if required, can be introduced via a precision leak valve, manually controllable down to a few 10^{-10} mbar l/s. An internal tube leads the gas from the leak valve to the electron gun (Fig. 2a), where the injected oxygen realises depoisoning of the cathode, see further [20].

2.7. Power supplies

All power supplies except for the trap tubes and outer barrier tubes are static. The power supplies for cathode heating, Wehnelt electrode, electron suppressor and collector are on gun platform potential. Any current leaving the platform is considered as loss current and is limited to 2.5 mA to protect the system.

Abrupt temperature changes may provoke breaking of the cathode crystal as discussed in [20] and therefore a buffer capacity is inserted. At REXEBIS on the other hand a battery backup in combination with an electronics card provides controlled ramping up and down functionality and ensures slow temperature changes at REXEBIS, also in case of power cuts. At TwinEBIS the cathode heating is manually regulated. Four TREK 601B amplifiers are connected to the pulsed drift tubes. The amplifiers can provide 0–1 kV and 20 mA peak current, with a slew rate > 35 V/us and are connected to a National Instruments (NI) PXI system including an FPGA card.

Fig. 5 shows the layout of the power supply configuration for TwinEBIS. The whole EBIS is installed on a high voltage platform to allow for ion extraction at higher energies at a later stage.

2.8. Ion beam diagnostics

The ion beam diagnostics is presently limited to a Multi-Channel Plate (MCP) placed after the extraction electrode at ground potential. It is a 25 mm diameter Chevron type MCP from ProxiVision with a P43 phosphor screen. Used in Time-of-Flight mode the extracted ion pulse length for different extraction modes can be recorded. The front of the MCP is negatively charged to around −1.5 kV, hence avoiding the repulsion of extracted low energy ions. The MCP anode current, transformed via a 550 Ω resistor to voltage, is recorded by an FPGA connected to the control system. Via a viewport with Kodial® glass at the MCP cross the cathode can be inspected visually and temperature measurements be carried out using a pyrometer. The window is protected by a manual shutter when not in use to avoid activation of colour centres in the glass by impinging ions and X-rays.

2.9. Control system

The TwinEBIS control system consists of a cRIO unit by National Instruments handling static power supplies and vacuum readout, and a NI-PXI in combination with an FPGA controlling the pulsed drift tubes and the MCP DAQ. Both units use analogue I/O and are remotely controlled via Ethernet. The static power supplies are connected via RS232 to the cRIO which currently has two 16-bit I/O modules connected and one relay card. The arbitrary functions from the PXI

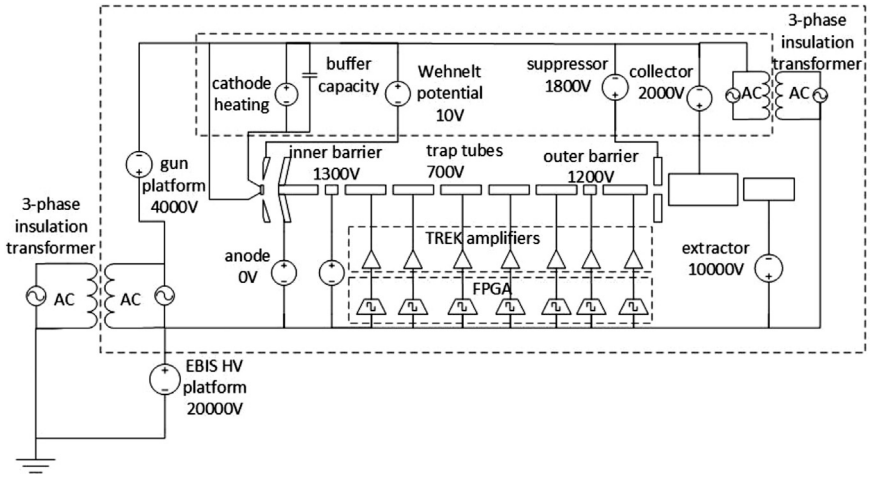

Fig. 5. Scheme of the TwinEBIS power supplies with typical operating voltages indicated.

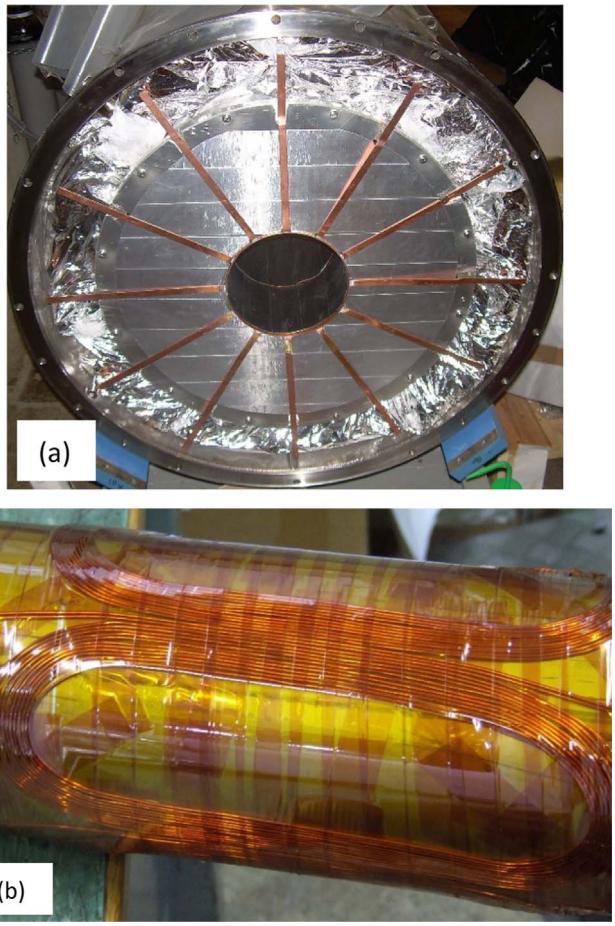

Fig. 6. (a) Cryogenic intervention at the TwinEBIS magnet with the iron shield dismounted (two bars at the bottom remaining) and the cryostat partly open. The photo shows the addition of radial copper strips that effectively connects the liquid nitrogen jacket to the 80 K tube, which shields the liquid helium jacket from the room temperature bore tube. (b) Photo of the transverse steering coils located between the cooling mantle and the solenoid bore as of 2016.

system have 12-bit resolution and the MCP is read out by an FPGA module utilised together with a digitiser adapter module.

3. Re-commissioning of the solenoid

Bringing TwinEBIS to operation required several actions targeting cryogenics, the magnetic field and alignment aspects. After relocation to CERN the TwinEBIS solenoid suffered from excessive helium boil-off from the magnet cryostat, also experienced at the REXEBIS solenoid after multiple vacuum bake-out cycles. The helium losses were minimised by dismounting the magnet cryostat and improving the heat isolation, and particularly improving the temperature distribution on the liquid nitrogen shield at the bore (Fig. 6a). The intervention on the TwinEBIS cryostat is described in [28]. Now the nitrogen and helium jackets are refilled with 8 and 12 d intervals, respectively. Until now TwinEBIS, and REXEBIS as well, do not feature transverse steering coils along the beam axis for adjustment of the electron beam position. Instead the gun and collector crosses, with intermediate drift tube structure, can be displaced transversally with respect to the main solenoid in order to align the structure, and as a consequence the electron beam, to the magnetic field. The future experimental program at TwinEBIS includes operation of high compression Brillouin flow electron guns, which are known to be much more sensitive to any field misalignment. For fine field adjustment the TwinEBIS magnetic optics has therefore been extended by three sets of steering coils with a horizontal and a vertical pair each, see Fig. 6b. The coil lengths are 20 cm in the injection and extraction region and 80 cm in the centre, which at full field strength of 1 mT can displace the electron beam by approximately 0.2, 0.4 and 0.2 mm, respectively.

The dismantling of the iron shield and internal parts of the magnet may have affected the alignment of the magnetic field. A precise alignment is crucial to avoid parts of the electron beam being misguided and create loss current as described above. After the cryogenic intervention the magnet was re-assembled in several steps assuring a high field quality. The parallelism of the iron yoke end plates was first verified to be 0.75 ± 0.2 mrad by means of a telescope on axis and mirrors attached to the flanges. Afterwards the cryostat was radially pre-centred with respect to the iron yoke, more specifically to the 150 mm diameter holes in the cylindrical end plates of the iron yoke, with a precision of ± 0.2 mm. The field of the solenoid was mapped with a rotating Hall probe every few centimetres along the geometrical axis given by the bore holes, similar to the procedure described in [22]. After mapping the trace of a central field line the solenoid inside of the cryostat was adjusted using axial and radial positioning knobs. Thereafter the mapping and repositioning process was iterated until the central field line was aligned within a cylinder with a 0.1 mm radius from the geometrical axis over a length of 750 mm in both directions from the centre of the solenoid. The final field deviation along the z-axis is shown in Fig. 7. With this method the complete field line straightness is characterised and not only the field alignment at the bore edges, as done for most EBIS devices. Secondly, by rotating the tube enclosing the Hall probe and measuring the field transversally in four directions (up, down, left and right) such that the mean is obtained, possible non-straightness of the tube sustaining the Hall probe could be annulled. The tube sag could be established with optical measurements.

4. Electron beam simulations

A high precision dimension control of the actual gun geometry in an assembled state was performed, see Fig. 8. Based on these data a gun model was implemented in TRAK from Field Precision [29]. Numerical simulations were then used in order to create a predictive model of TwinEBIS explaining the experimental results and easing the machine development. The position of the collector assembly and internal distances therein were also taken from the measurement. Simulations of the existing geometry showed a gun perveance of 2.95 uA/V$^{3/2}$. Lower simulated and measured values have been reported for REXEBIS [30] which is due to a different cathode-anode distance.

In order to reach the design value of 0.5 A for the electron gun while operating it in the space-charge limited mode (i.e. in the Child-Langmuir regime), extreme cathode temperatures above 2000 K are necessary, which are not compatible with a reliable long-term operation. Thus, we run the electron gun with high voltages (> 3.5 kV),

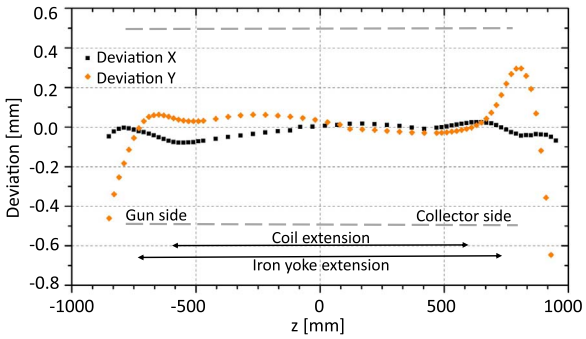

Fig. 7. Measured excursion of the central field line inside TwinEBIS after alignment of the magnet cryostat within the iron shield. The gravitational sag has not been compensated for in the plot, thus the fall-off in vertical direction outside the shield. The dashed line indicates the specified maximum field-line excursion over a range of ± 850 mm.

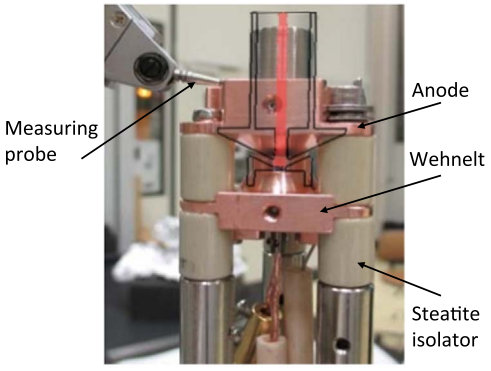

Fig. 8. The TwinEBIS electron gun being measured in assembled state at the metrology section. The dimensions and relative alignment were verified with 1.9 μm+L/250 mm precision (L typically 5–10 mm). The Wehnelt and anode cross sections (black), together with the electron beam (red), are indicated in the figure. (For interpretation of the references to color in this figure legend, the reader is referred to the web version of this article.)

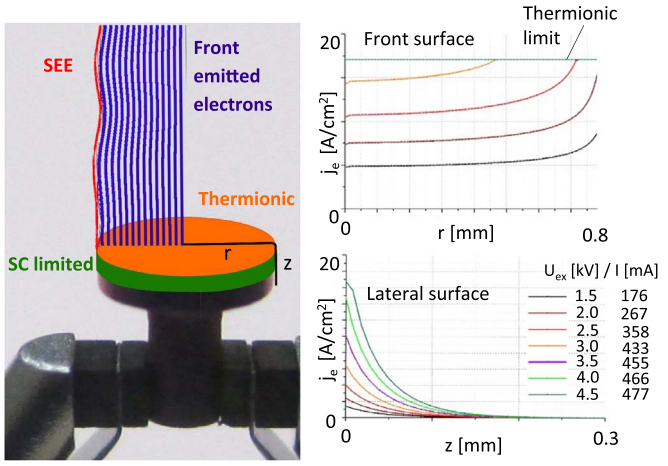

Fig. 9. Distribution of emission modes on the cathode at T_c=2100 K for a range of extraction voltages up to 4.5 kV. Local emission current densities are shown for front and side surfaces on the inserts. The trajectories are shown for the highest applied voltage of 4.5 kV corresponding to 477 mA total emission with the front surface operating in the thermionic limit while Side Emitted Electrons (SEE) are emitted in the space-charge limited mode. Note that the cathode rim is excluded in the inserts as the emission from sharp curved surfaces in the simulation program may produce artifacts in the local current density [32].

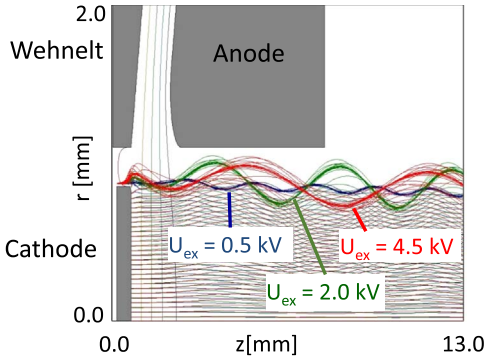

Fig. 10. Trajectories of side-emitted electrons at three different extraction voltages plotted in axisymmetric geometry.

where the electron emission from the front surface is no longer limited by space charge, but rather by the emission density at the given temperature, work function and voltage (i.e. in the thermionic regime). To accommodate this in the simulations we have further refined the cathode emission model as a second step. We have established realistic maximum emission current densities based on the emission current measurements for different temperatures. The maximum emission current densities were adjusted such that simulated extracted currents at maximum voltage (well in the thermionic regime) were equal to the measurements. With a pre-set maximum emission density the simulated cathode operates in a combined mode. Some emission nodes reach maximum current density and work in the thermionic regime while less dense emission nodes are space-charge limited. The emission mode of a specific node is defined by the local extracting electric field.

Apart from limited front-emission, another factor needs to be considered in the simulations. Due to the gap between the cathode and the Wehnelt electrode, electrons are extracted from the side of the cathode [31]. The side-surface is chemically similar to the front, although with a different crystal index. As it is unknown, in the simulations we have assumed the same work function for the side as for the front, possibly over-estimating side emission. The side surface is exposed to a much weaker electric extraction field and therefore remains in the space-charge limited regime at all applied extraction voltages up to 4.5 kV. Despite of lower extracting field the side-surface emission can account for up to 10% of the total emitted current at highest applied voltages, and exceed this value if the front surface is at the emission limit. The side emission is also decisive as these electrons are emitted with substantial transverse momentum and are very likely to behave differently from the main part of the beam creating a beam halo, stray trajectories and thus eventually loss current.

Fig. 9 shows the contribution of front and side-surfaces to the total emission. The inserts show that while the front emission undergoes a transition from space-charge to thermionic limitation for increasing extraction voltages, the side emission always remains in the space-charge regime.

In Fig. 10 the electron beam propagation in the gun region is shown for different extraction voltages. Emission at the front surface ranges from fully space-charged limited at 0.5 kV to thermionically limited emission at 4.5 kV. The ripple amplitude and frequency of the SEE changes with the extraction voltage and extracted current. The SEE remain in the space-charge limited mode at all extraction voltages.

In order to overcome difficulties due to the large aspect-ratio when tracing the beam through the solenoid, we have made use of a technique that divides the volume into sub-domains and subsequently performs smooth splicing of the solutions [33]. In doing so, the simulated electron beam can propagate into the high magnetic-field-region and to the collector. Such simulations are essential for identifying potential electron reflections at the magnetic field gradient, or electron back-streaming from the collector due to secondary processes.

Propagating the beam into the full magnetic field allowed us to estimate the electron current density in the ionisation region. A beam radius of 275 μm was found, corresponding to a density of 210 A/cm^2 in the full 2 T field for a thermionically limited beam of 0.5 A at 4.4 keV electron energy. The beam was further propagated to the collector were secondary processes were studied. Using techniques described in [33] we have investigated whether paraxial Elastically Reflected Primary Electrons (ERPE) or Back Scattered Electrons (BSE) with high transverse momentum can re-enter the ionisation region and create loss current. The simulation results shown in Fig. 11a indicate that indeed both the ERPE and BSE create loss current on the last drift tube. A loss current in the range of 1 mA for a total electron beam current of ~400 mA was experimentally observed. Furthermore, in this simulation case the position of the collector assembly with respect to the solenoid field was not optimal, and resulted in primary electrons (PE) hitting the suppressor and the edge of the collector. The ideal trajectories calculated for a properly placed but otherwise identical TwinEBIS collector are shown in Fig. 11b. The difference in axial alignment relative to the main solenoid in Fig. 11a and 11b is 3 mm.

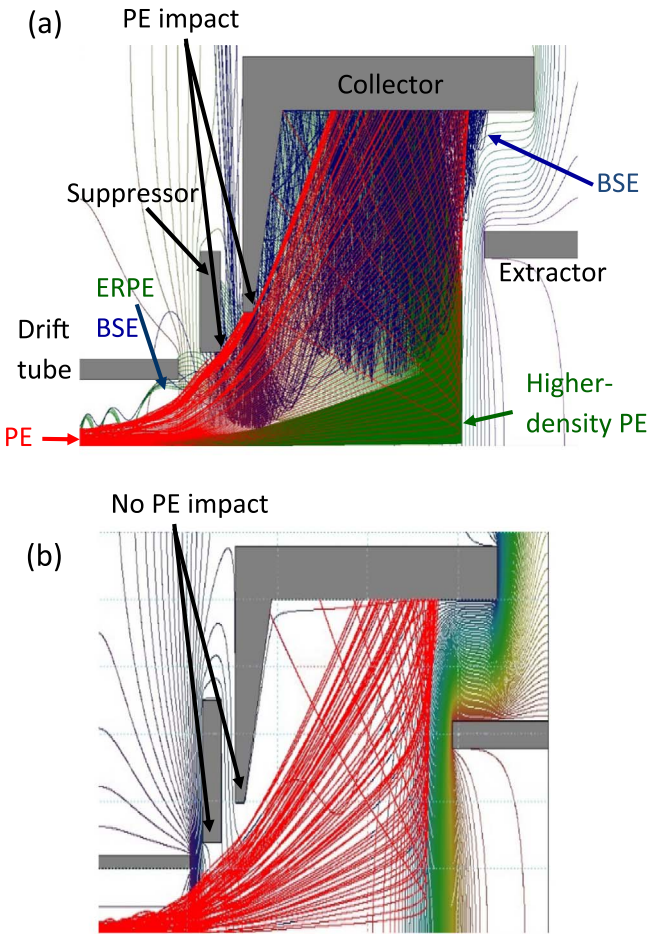

Fig. 11. (a) Electron beam propagation inside the TwinEBIS collector. In this case, the current was 477 mA, the energy at the last drift tube 5.5 keV and the impact energy at the collector 2 keV. The primary electrons (PE) (red) generate back-scattered electrons (BSE) (blue) at the impact surface. The core of the beam, simulated with higher trajectory density (green), is used to establish the fraction of elastically reflected primary electrons (ERPE) more precisely. PE beam impinging on the suppressor and the edge of the collector has motivated us to move the collector assembly closer to the main solenoid as shown in (b). Here the flow of the PE (red) is shown in an axial geometry for an ideal placement in the magnetic field. Note that neither BSE, nor higher-density trajectories, are included in this case. (For interpretation of the references to color in this figure legend, the reader is referred to the web version of this article.)

5. Summary

The TwinEBIS solenoid has been transferred to CERN where it was modified to increase the liquid helium holding time. It was equipped with an internal structure very much resembling that of REXEBIS, and was thereafter commissioned. TwinEBIS now serves as a test bench for REXEBIS improvements, in particular for tests of higher performing electron guns also to be used at cancer therapy treatment facilities. The iron-shielded solenoid houses a semi-immersed electron gun. A current density of 210 A/cm^2 is expected in the trapping region, where typical beam energies ranges from 3 to 6 keV. The collector has an open geometry and absorbs the electrons on a cylindrical non-conical surface. The good vacuum is obtained with high-compression turbo-molecular drag pumps at the gun and collector crosses, in combination with NEG strips surrounding the drift tube structure.

Extensive electron simulations have been performed. The simulation geometry has been based on high precision dimension control of the actual electron gun. Electron emission from the side of the cathode and realistic work functions have been implemented. The gun was simulated in the combined emission regime, i.e. part of the surface was thermionically emission limited while the other part was space-charge limited. Besides the gun region, the multi-domain solving and splicing technique was used to study the beam optics further downstream. The current density in the trapping region was calculated by propagating the beam into the high field region. The beam was further tracked to the collector region in order to study its absorption and losses due to elastic and inelastic scattering processes. These studies predicted some losses observed in experiments and were used to benchmark modifications aiming at suppressing losses.

A method for alignment of the magnetic field to the optical axis has been described. The method maps the field along the full solenoid length and not only at the bore ends, and eliminates errors due to possible bending of the probing arrangement. The magnetic field has been aligned with the geometrical axis with a precision of ± 0.1 mm over a length of ± 750 mm. In a second paper [20] further results from the commissioning of TwinEBIS, cathode tests and ion extraction are presented.

Acknowledgement

For this work A. Shornikov has been supported by a Marie Curie Initial Training Network Fellowship of the European Community's FP7 Programme under contract number (PITN-GA-2010-264330-CATHI). J. Pitters is supported by a Marie Skłodowska-Curie Innovative Training Network Fellowship of the European Commission's Horizon 2020 Programme under contract number 642889 MEDICIS-PROMED. Working on this project A. Shornikov received funding from the European Union's Horizon 2020 Research and Innovation Programme under grant agreement No 654002.

References

[1] F. Wenander et al., REXEBIS – a charge state breeder for the REX-ISOLDE post accelerator, in: Proceedings of the 6th European Particle Accelerator Conference, Stockholm, Sweden, 1999, pp. 1412–1414. ⟨http://accelconf.web.cern.ch/AccelConf/e98/PAPERS/MOP05A.PDF⟩.
[2] F. Wenander, Charge breeding of radioactive ions with EBIS and EBIT, J. Instrum. (2010) 32. http://dx.doi.org/10.1088/1748-0221/5/10/C10004 (5 C1004).
[3] F. Ames et al., The REX-ISOLDE Facility: Design and Commissioning Report, CERN-2005-009, pp. 113. ⟨http://cds.cern.ch/record/895873/files/CERN-2005-009.pdf?version=1⟩.
[4] O. Kester, et al., Accelerated radioactive beams from REX-ISOLDE, Nucl. Instrum. Methods B 204 (2003) 20–30. http://dx.doi.org/10.1016/S0168-583X(02)01886-4.
[5] D. Voulot, et al., Radioactive beams at REX ISOLDE: present status and latest developments, Nucl. Instrum. Methods B 266 (2008) 4103–4107. http://dx.doi.org/10.1016/j.nimb.2008.05.129.
[6] P. van Duppen, K. Riisager, Physics with REX-ISOLDE: from experiment to facility, J. Phys. G: Nucl. Part. Phys. 38 (2011) 24. http://dx.doi.org/10.1088/0954-3899/38/2/024005 (024005).
[7] S. Schwarz, et al., A high-current electron gun for the electron beam ion trap at the National Superconducting Cyclotron Laboratory, Rev. Sci. Instrum. 85 (2014) 02B705. http://dx.doi.org/10.1063/1.4827109.
[8] S. Kondrashev et al., First charge breeding results at CARIBU EBIS, in: AIP Conference Proceedings, vol. 1640, 2015, pp. 54–67. ⟨http://dx.doi.org/10.1063/1.4905400⟩.
[9] F. Ames, et al., Charge state breeding experiences and plans at TRIUMF, Rev. Sci. Instrum. 87 (2016) 02B501. http://dx.doi.org/10.1063/1.4932317.
[10] J. Kim et al., An EBIS system for rare isotope science project in Korea, in: AIP Conference Proceedings, vol. 1640, 2015, pp. 38-43. ⟨http://dx.doi.org/10.1063/1.4905398⟩.
[11] A. Pikin, et al., RHIC EBIS: basics of design and status of commissioning, J. of Instrum. 5 (2010) C09003. http://dx.doi.org/10.1088/1748-0221/5/09/C09003.
[12] S. Schwarz, A. Lapierre, Recent charge-breeding developments with EBIS/T devices, Rev. Sci. Instrum. 87 (2016) 02A910. http://dx.doi.org/10.1063/1.4933033.
[13] R. Catherall, et al., An overview of the HIE-ISOLDE design study, Nucl. Instrum. Methods B 317m (2013) 204–207. http://dx.doi.org/10.1016/j.nimb.2013.07.030.
[14] A. Shornikov, et al., Design study of an upgraded charge breeder for ISOLDE, Nucl. Instrum. Methods B 317 (2013) 395–398. http://dx.doi.org/10.1016/j.nimb.2013.06.030.
[15] G.I. Kuznetsov, IrCe cathodes for EBIS, J. Phys. Conf. Ser. 2 (2004) 35–41. http://dx.doi.org/10.1088/1742-6596/2/1/005.
[16] E. Beebe et al., Reliable operation of the Brookhaven EBIS for highly charged ion production for RHIC and NSRL, in: AIP Conference Proceedings, vol. 1640, 2015, pp. 5–11. ⟨http://dx.doi.org/10.1063/1.4905394⟩.
[17] S. Kondrashev et al., Commisioning of CARIBU EBIS charge breeder, HIAT 2012,

Chicago, 2012. ⟨http://accelconf.web.cern.ch/AccelConf/HIAT2012/papers/web02.pdf⟩.
[18] L. Brillouin, A theorem of Larmor and its importance for electrons in magnetic fields, Phys. Rev. 67 (1945) 260–266. http://dx.doi.org/10.1103/PhysRev.67.260.
[19] R. Mertzig et al., A high-compression electron gun for C^{6+} production: concept, simulations and mechanical design (2017) this issue. ⟨http://dx.doi.org/10.1016/j.nima.2016.12.036⟩.
[20] R. Mertzig et al., The TwinEBIS setup: commissioning results, to be published.
[21] E.D. Donets, et al., A study of electron strings and their use for efficient production of highly charged ions, Rev. Sci. Instrum. 71 (2) (2000) 896–898. http://dx.doi.org/10.1063/1.1150325.
[22] F. Wenander et al., REXEBIS - the electron beam ion source for the REX-ISOLDE project, CERN-OPEN-2000-320. ⟨http://cds.cern.ch/record/478399/files/open-2000-320.pdf⟩.
[23] F. Wenander et al., REXEBIS, design and initial commissioning results, in: AIP Conference Proceedings, vol. 572, 2001, pp. 59–73. ⟨http://dx.doi.org/10.1063/1.1390100⟩.
[24] M. Gesley, L.W. Swanson, A determination of the low work function plans of LaB_6, Surf. Sci. Lett. 146 (1984) 583–599. http://dx.doi.org/10.1016/0167-2584(84)90778-3.
[25] W. Pirkl, RF measurements on CRYSIS, Manne Siegbahn Laboratory Annual Report 1997, pp.13–16. ⟨http://www.msl.se/ANNREP/ar97.pdf⟩.
[26] F. Wenander, et al., The REX-ISOLDE charge breeder as an operational machine, Rev. Sci. Instrum. 77 (2006). http://dx.doi.org/10.1063/1.2149384 (03B104-1-5).
[27] C. Benvenuti, P. Chiggiato, Pumping characteristics of the St707 nonevaporable getter (Zr 70 V 24.6-Fe 5.4 wt%), J. Vac. Sci. Technol. A 14 (1996) 3278–3282. http://dx.doi.org/10.1116/1.580226.
[28] T. Berg, Installation and commissioning of an electron beam ion source (Master of Science Thesis), Department of Mechanical Engineering in the University of Oulu, Finland, 2011.
[29] S. Humphries, TRAK charged particle tracking in electric and magnetic fields, Computational accelerator physics, in: AIP Conference Proceedings, vol. 297, 1993, pp. 597–604. ⟨http://dx.doi.org/10.1063/1.45318⟩.
[30] B. Wolf, et al., Commissioning results from the REXEBIS charge breeder, Rev. Sci. Instrum. 73 (2002) 682–684. http://dx.doi.org/10.1063/1.1427035.
[31] V.P. Yakovlev et al., Electron gun for a high-power X-band magnicon amplifier, in : Proceedings of the Particle Accelerator Conference, 1997, pp. 3186-3188. ⟨http://accelconf.web.cern.ch/accelconf/pac97/papers/pdf/7p054.pdf⟩.
[32] S. Humphries, Numerical modeling of space-charge-limited charged-particle emission on a conformal triangular mesh, J. Compd. Phys. 125 (1996) 488–497. http://dx.doi.org/10.1006/jcph.1996.0110.
[33] R. Mertzig et al., Electron beam simulation from gun to collector: towards a complete solution, in: AIP Conference Proceedings, vol. 1640, 2015, pp. 28–37. ⟨http://dx.doi.org/10.1063/1.4905397⟩.